Singularity Conditions of Concentric Tube Robots

Federico Zaccaria, Edoardo Idá, Sébastien Briot

Singularity Conditions of Concentric Tube Robots

Federico Zaccaria[1,3], Edoardo Idà[1], and Sébastien Briot[2]

[1] DIN, University of Bologna, Bologna, Italy
{federico.zaccaria3,edoardo.ida2}@unibo.it
[2] CNRS, Laboratoire des Sciences du Numérique de Nantes (LS2N), Nantes, France,
Sebastien.Briot@ls2n.fr
[3] École Centrale de Nantes, Laboratoire des Sciences du Numérique de Nantes (LS2N), Nantes, France

Abstract. This paper derives singularity conditions for concentric tube robots (*CTRs*). To the scope, we build the *CTR* geometrico-static model using discretization techniques, which are suitable for several currently-used *CTRs* models. Then, we obtain singularity conditions by performing a linearization of the geometrico-static model. We define Type-1 and Type-2 singularities, which are related to the unsolvability of the inverse and forward kinematostatic problems, respectively. Moreover, we also show the link between Type-2 singularities and *CTR* equilibrium stability. A case study with a two-tube *CTR* is proposed to illustrate our results.

Keywords: Concentric Tube Robots, Singularity Conditions, Equilibrium Stability

1 Introduction

Continuum robots (*CRs*) are manipulators usually made by flexible components and designed to achieve safe human-robot interactions [5]. *CRs* promise significant advantages in robotized surgery because of their inherent flexibility and the ability to move and traverse unstructured confined spaces. In this direction, concentric tube robots (*CTRs*) are a class of continuum robots typically made of superelastic pre-curved tubes assembled in a concentric arrangement [7], which have been adopted for different surgical applications (e.g. [19]).

Because of their promising features, *CTRs* received great attention from the scientific community [11]. Modelling [15], design [18], and control [20] are among the most investigated aspects, and we address the interested reader to specialized review papers [1]. Equilibrium stability assessment is a crucial aspect of *CTRs*, since it impacts both usability and controllability: as the tubes rotate and translate with respect to each other, elastic potential energy accumulates until an unstable configuration is met, and the energy is released with a dangerous snapping [9]. To address the problem of elastic instabilities, a first approach is based on stable-path motion planning [3]. Alternatively, design considerations such as

the use of transverse anisotropy [16], or design rules [10] help to avoid elastic instabilities. Singularities of *CTR* were rarely investigated, and are preliminary identified by singular value decomposition of the models Jacobian matrix [6]. However, this procedure does not allow singularities classification, which is intimately linked to what cause them, and neglects the potential links between them and equilibrium stability [22],[4].

The novel contribution of this paper is the definition and classification of singularity conditions for *CTRs*. While rigid-links-robot singularities are investigated by using of geometric approaches, the elastic nature of *CTRs* requires more complex tools, and our analysis is based on energetic considerations. We first obtain the *CTR* geometrico-static model by using discretization strategies, as it is compatible with several currently employed *CTR* models. Then, we derive singularity conditions by studying the kinematostatic model of *CTRs*, obtained as a linearization of the geometrico-static model. In analogy to [4], we will show that the forward kinemato-static problem singularities define stable-to-unstable *CTR* transitions.

The paper is structured as follows. Section 2 describes the *CTR* modelling framework based on discretization approaches, and Section 3 derives singularity conditions and discusses equilibrium stability assessment. Then, Section 4 proposes a case study to illustrate singularities, and compares the results with state-of-the-art results. Finally, conclusions and drawn in Section 5.

2 Modelling

In this Section, we derive the geometrico-static model of a *CTR* based on energetic considerations. We first obtain the tubes energy, and then we consider the full *CTR* energy to derive the *CTR* geometrico-static model.

2.1 Tubes energy

Let us consider a *CTR* made by n concentric tubes (Fig. 1(a)). A fixed frame $\mathcal{F}_0$ is attached to the robot base, and the coordinate s is used to parametrize the robot centerline. We use i as the index representing the i-th tube, numbered from the innermost to the outermost. The length of the i-th tube, measured from the arc length $s = 0$, is L_i. The tubes are actuated at the coordinate $s = -\beta_i$ in translation and rotation: we name θ_{0i} the rotation of the tube's base, and β_i is called transmission length.

As done in [13], a frame $\mathcal{F}_b$ is attached to the robot centerline at each s, and $\mathbf{p}(s)$ defines the position of $\mathcal{F}_b$ with respect to (w.r.t.) $\mathcal{F}_0$. Then, the orientation of $\mathcal{F}_b$ is described by $\mathbf{R}_b$, that is a rotation matrix obtained by sliding the base frame orientation matrix along the robot centerline without any rotation about the local z axis, assuming the z axis to be aligned with the centerline tangent vector. Since the tubes are concentric, the position of the i-th tube is $\mathbf{p}_i(s) = \mathbf{p}(s)$. However, the concentric tube arrangement let each tube to be free to twist around the local z axis of an angle $\theta_i(s)$ (see Fig. 1(b)). Thus, we can

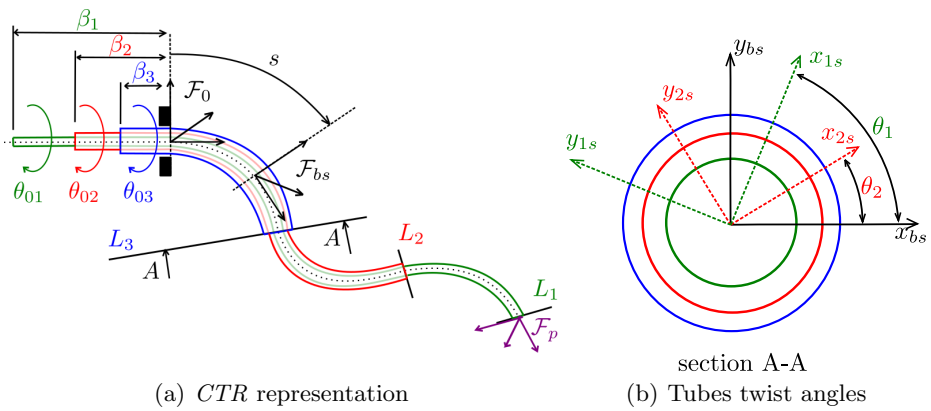

(a) *CTR* representation

section A-A

(b) Tubes twist angles

Fig. 1: Representation of a *CTR*: relevant configuration variables are displayed in (a), and the tubes twist angles are illustrated in (b).

recover the i-th tube orientation w.r.t. $\mathcal{F}_0$ as $\mathbf{R}_i(s) = \mathbf{R}_z(\theta_i(s))\mathbf{R}_b(s)$, where $\mathbf{R}_z$ is an elementar rotation around z. Then, we consider $\mathbf{u}_b(s)$, which represents the angular rate of change of $\mathbf{R}_b(s)$ w.r.t. s. We can recover the i-th tube curvature $\mathbf{u}_i(s)$ as [13]:

$$\mathbf{u}_i(s) = \mathbf{R}_z^T(\theta_i(s))\mathbf{u}_b(s) + \theta_i'(s)\mathbf{e}_z \tag{1}$$

where $(.)' = d/ds$, and $\mathbf{e}_z = [0;0;1]$. In the following, the variables explicit dependence from s is dropped for brevity sake.

In order to derive the *CTR* geometrico-static model, let us consider the deformation energy of the tubes V_t. By assuming linear elasticity, and by neglecting shear and extensibility on the tubes, we can compute V_t as [17]:

$$V_t = \sum_{i=1}^{n} V_i; \quad V_i = \frac{1}{2}\int_{L_{i-1}}^{L_i} \left(\sum_{j=1}^{m} \left(\mathbf{u}_j - \mathbf{u}_j^*\right)^T \mathbf{K}_t \left(\mathbf{u}_j - \mathbf{u}_j^*\right)^T \right) ds \tag{2}$$

where $L_0 = 0$, $m = n + 1 - i$, $\mathbf{u}_i^*$ is the initial tube precurvature, $\mathbf{K}_i = \text{diag}(k_{bi}, k_{bi}, k_{ti})$, is the local stiffness matrix, k_{bi} the flexural stiffness, and k_{ti} the torsional stiffness of the i-th tube. By introducing Eq. (1), into Eq. (2) we have:

$$V_i = \frac{1}{2}\int_{L_{i-1}}^{L_i} \sum_{j=1}^{m} \left(\mathbf{R}_z^T(\theta_j)\mathbf{u}_b + \theta_j'\mathbf{e}_z - \mathbf{u}_j^*\right)^T \mathbf{K}_j \left(\mathbf{R}_z^T(\theta_j)\mathbf{u}_b + \theta_j'\mathbf{e}_z - \mathbf{u}_j^*\right)^T ds \tag{3}$$

Thus, the tubes energy depends on $\mathbf{u}_b$, all the θ_i of the tubes and the actuated lengths L_i.

2.2 *CTR* energy

In order to deduce *CTR* energy, some configuration variables classification is necessary. First, we introduce the vector $\mathbf{q}_a \in \mathbb{R}^{2n}$ to collect the actuated vari-

ables (base rotation θ_{i0} and length L_i of each tube, two motors for each tube). Then, we introduce $\mathbf{q}_p = [\mathbf{p}_p, \boldsymbol{\alpha}_p] \in \mathbb{R}^6$ to represent the *CTR* tip pose: $\mathbf{p}_p \in \mathbb{R}^3$ is the tip position, and $\boldsymbol{\alpha}_p \in \mathbb{R}^3$ are three orientation angles of the tip that define $\mathbf{R}_p = \mathbf{R}_p(\boldsymbol{\alpha}_p)$. For later convenience, we introduce $\mathbf{q}_c$ the set of controlled variables: we assume to have the same number of controlled and actuated variables, and thus $\mathbf{q}_c \in \mathbb{R}^{2n}$. In general, $\mathbf{q}_c$ is a subset of $\mathbf{q}_p$, and the remaining tip variables are stacked into $\mathbf{q}_d \in \mathbb{R}^{6-2n}$. To evaluate the *CTR* energy, we consider the energy associated with a tip force $\mathbf{f}_p$, constant w.r.t. $\mathcal{F}_0$, that is[4].

$$V_{tip} = -\mathbf{f}_p^T \mathbf{p}_p \tag{4}$$

and the total *CTR* potential energy is obtained as:

$$V_{tot} = V_{tip} + V_t \tag{5}$$

Although we introduced $\mathbf{q}_p$ to represent the *CTR* tip pose, we can also recover the *CTR* tip pose as inner tube distal section pose:

$$\mathbf{g}_{tip} = \mathbf{g}_0 + \int_0^{L_1} \mathbf{g}\tilde{\boldsymbol{\xi}} ds; \quad \tilde{\boldsymbol{\xi}} = \begin{bmatrix} \widehat{\mathbf{u}}_1 & \mathbf{e}_z \\ \mathbf{0} & 0 \end{bmatrix} \tag{6}$$

with $\widehat{\mathbf{u}}_1 \in so(3)$ is the skew-symmetric matrix obtained from $\mathbf{u}_1$, and $\mathbf{g}, \mathbf{g}_0, \mathbf{g}_{tip} \in SE(3)$ are the matrices expressing the pose the first tube at s, the pose of the base frame, and the tip pose, respectively. Thus, since $\mathbf{q}_p$ must represent the same pose as the one obtained in Eq. (6), the following constraint is introduced:[5]

$$\boldsymbol{\Phi} = \begin{cases} \mathbf{p}_p - \mathbf{p}_{tip} = \mathbf{0} \\ \check{(}\mathbf{R}_p^T \mathbf{R}_{tip} - \mathbf{R}_{tip}^T \mathbf{R}_p\check{)} = \mathbf{0} \end{cases}, \ \boldsymbol{\Phi} \in \mathbb{R}^6 \tag{7}$$

where $\mathbf{p}_{tip}, \mathbf{R}_{tip}$ are the tip position and orientation obtained from Eq.(6), and the operator $\check{(.)}$ extracts the three independent components from its argument.

2.3 Geometrico-static model

CTRs equilibrium configurations are associated with critical points of the robot energy V_{tot} [17]. The function V_{tot} depends on $\mathbf{q}_a, \mathbf{q}_p$, and the continuous functions $\mathbf{u}_b$ and θ_i. Moreover, constraints $\boldsymbol{\Phi}$ must be enforced. Discretization techniques offers a straightforward way to numerically identify critical points of V_{tot} [2], and a finite set of discretization coordinates $\mathbf{q}_e \in \mathbb{R}^m$ is introduced to parametrize the tubes elastic deformations [2]. For convenience, we define $\mathbf{q}_u = [\mathbf{q}_e, \mathbf{q}_d] \in \mathbb{R}^{m+6-2n}$ to collect the uncontrolled variables after the discretization of the tubes, and $\mathbf{x} = [\mathbf{q}_u, \mathbf{q}_c] \in \mathbb{R}^{m+6}$ the non actuated variables.

[4]Generic concentrated loads or distributed load are neglected for simplicity, but their inclusion is possible. Moments which are not conservative are not considered.

[5]Instead of considering $\mathbf{q}_p$ as independent variables, the tip pose could be obtained directly by integration of Eq. (6). However, the introduction of $\mathbf{q}_p$ simplifies the following singularity derivation.

Please note that this way of parametrizing the *CTR* is true regardeless of the discretization technique employed.

After the discretization process, $V_{tot} = V_{tot}(\mathbf{q}_a, \mathbf{x})$ and $\boldsymbol{\Phi} = \boldsymbol{\Phi}(\mathbf{q}_a, \mathbf{x})$. Due to the presence of constraints, critical points of V_{tot} are characterized by Lagrange conditions [12]: assuming $\nabla_{\mathbf{x}}\boldsymbol{\Phi}$ is full row rank, $\mathbf{x}$ is a critical point of V_{tot} if there exists a vector of Lagrange multipliers $\boldsymbol{\lambda} \in \mathbb{R}^6$ such as:

$$\mathbf{G}(\mathbf{q}_a, \mathbf{x}, \boldsymbol{\lambda}) = \begin{cases} \nabla_{\mathbf{x}} V_{tot} + \nabla_{\mathbf{x}}\boldsymbol{\Phi}^T \boldsymbol{\lambda} = \mathbf{0} \\ \boldsymbol{\Phi} = \mathbf{0} \end{cases} \tag{8}$$

Equation (8) represents the geometrico-static model of a *CTR*, which is an undetermined system of $m+6+6$ system of equations in $2n+m+6+6$ unknowns. As in [4], forward and inverse problems are stated in a unified formulation:

$$\mathbf{F}(\mathbf{q_a}, \mathbf{x}, \boldsymbol{\lambda}) = \begin{cases} \nabla_{\mathbf{x}} V_{tot} + \nabla_{\mathbf{x}}\boldsymbol{\Phi}_p^T \boldsymbol{\lambda} = \mathbf{0} \\ \boldsymbol{\Phi} = \mathbf{0} \\ \mathbf{e} = \mathbf{0} \end{cases} \tag{9}$$

where $\mathbf{e} = \mathbf{q}_a - \mathbf{q}_a^d$ for the forward problem, $\mathbf{e} = \mathbf{q}_c - \mathbf{q}_c^d$ for the inverse problem, and the superscript $(.)^d$ indicates a desired value. Eqs. (9) is a system of $2n + m + 6 + 6$ non-linear equations that can be solved with appropriate root-finding techniques [12] (e.g the Newton-Raphson method).

3 Singularity Conditions and Equilibrium Stability

To obtain singularity conditions and to assess equilibrium stability of *CTRs*, we linearize the *CTR* geometric static model (8) w.r.t. to the robot configuration variables to obtain the *CTR* kinematostatic model:

$$\begin{bmatrix} \mathbf{A}_1 \\ \mathbf{A}_2 \end{bmatrix} \Delta\mathbf{q}_a + \begin{bmatrix} \mathbf{U}_1 \\ \mathbf{U}_2 \end{bmatrix} \Delta\mathbf{q}_u + \begin{bmatrix} \mathbf{P}_1 \\ \mathbf{P}_2 \end{bmatrix} \Delta\mathbf{q}_c + \begin{bmatrix} \mathbf{G} \\ \mathbf{0} \end{bmatrix} \Delta\boldsymbol{\lambda} = \mathbf{0} \tag{10}$$

where:

- $\mathbf{A}_1 = \nabla_{\mathbf{q}_a}(\nabla_{\mathbf{x}}\mathcal{L})$, $\mathbf{U}_1 = \nabla_{\mathbf{q}_u}(\nabla_{\mathbf{x}}\mathcal{L})$, $\mathbf{P}_1 = \nabla_{\mathbf{q}_c}(\nabla_{\mathbf{x}}\mathcal{L})$
- $\mathbf{A}_2 = \nabla_{\mathbf{q}_a}\boldsymbol{\Phi}$, $\mathbf{U}_2 = \nabla_{\mathbf{q}_u}\boldsymbol{\Phi}$, $\mathbf{P}_2 = \nabla_{\mathbf{q}_c}\boldsymbol{\Phi}$, $\mathbf{G} = \nabla_{\boldsymbol{\lambda}}(\nabla_{\mathbf{x}}\mathcal{L})$

To verify if a configuration is stable, we compute the reduced Hessian matrix of the total potential energy as [21]:

$$\mathbf{H}^r = \mathbf{Z}^T \begin{bmatrix} \mathbf{P}_1 & \mathbf{U}_1 \end{bmatrix} \mathbf{Z} \tag{11}$$

where $\mathbf{Z}$ is the left nullspace of $\mathbf{G} \in \mathbb{R}^{(m+6)\times 6}$, that is $\mathbf{Z}^T\mathbf{G} = \mathbf{0}$. As long as $\nabla_{\mathbf{x}}\mathbf{G}$ is full rank, $\mathbf{Z} \in \mathbb{R}^{(m+6)\times m}$. A configuration is stable if $\mathbf{H}^r$ is positive definite [12].

Then, to obtain singularity conditions, we multiply the first set of rows in Eq.(10) by $\mathbf{Z}^T$ [4]:

$$\begin{bmatrix} \mathbf{Z}^T\mathbf{A}_1 \\ \mathbf{A}_2 \end{bmatrix} \Delta\mathbf{q}_a + \begin{bmatrix} \mathbf{Z}^T\mathbf{U}_1 \\ \mathbf{U}_2 \end{bmatrix} \Delta\mathbf{q}_u + \begin{bmatrix} \mathbf{Z}^T\mathbf{P}_1 \\ \mathbf{P}_2 \end{bmatrix} \Delta\mathbf{q}_c = \mathbf{0} \tag{12}$$

which can be rewritten in a more compact form:

$$\mathbf{A}\Delta\mathbf{q}_a + \mathbf{U}\Delta\mathbf{q}_u + \mathbf{P}\Delta\mathbf{q}_c = \mathbf{0} \tag{13}$$

with $\mathbf{A} = [\mathbf{Z}^T\mathbf{A}_1, \mathbf{A}_2]^T \in \mathbb{R}^{(m+6)\times 2n}$, $\mathbf{U} = [\mathbf{Z}^T\mathbf{U}_1, \mathbf{U}_2]^T \in \mathbb{R}^{(m+6)\times(m+6-2n)}$, and $\mathbf{P} = [\mathbf{Z}^T\mathbf{P}_1, \mathbf{P}_2]^T \in \mathbb{R}^{(m+6)\times 2n}$. Similarly to [4], we can formulate the inverse kinemato-static problem as:

$$\begin{bmatrix} \mathbf{A} & \mathbf{U} \end{bmatrix} \begin{bmatrix} \Delta\mathbf{q}_a \\ \Delta\mathbf{q}_u \end{bmatrix} = \mathbf{T}_1 \begin{bmatrix} \Delta\mathbf{q}_a \\ \Delta\mathbf{q}_u \end{bmatrix} = \mathbf{P}\Delta\mathbf{q}_c \tag{14}$$

Matrix $\mathbf{T}_1$ is square of dimension $(m+6)\times(m+6)$ and, for given $\Delta\mathbf{q}_c$, we can invert $\mathbf{T}_1$ to evaluate $\Delta\mathbf{q}_a, \Delta\mathbf{q}_u$ as long as $\mathbf{T}_1$ is full rank. Rank deficiencies of $\mathbf{T}_1$, with $\mathbf{A}, \mathbf{U}$ full rank, are named *Type-1* singularities (according to the terminology of [8]). At the singular configuration, there exist non-null $\Delta\mathbf{q}_a, \Delta\mathbf{q}_u$ that leads to nulll $\Delta\mathbf{q}_c$. This physically means the exisistence of some direction for which the end-effector cannot move, even if non-null motor and tubes displacements occur. Then, we can formulate the forward kinemato-static problem as:

$$\begin{bmatrix} \mathbf{P} & \mathbf{U} \end{bmatrix} \begin{bmatrix} \Delta\mathbf{q}_c \\ \Delta\mathbf{q}_u \end{bmatrix} = \mathbf{T}_2 \begin{bmatrix} \Delta\mathbf{q}_c \\ \Delta\mathbf{q}_u \end{bmatrix} = \mathbf{A}\Delta\mathbf{q}_a \tag{15}$$

Matrix $\mathbf{T}_2$ is square of dimension $(m+6)\times(m+6)$ and, for given $\Delta\mathbf{q}_a$, we can invert $\mathbf{T}_2$ to evaluate $\Delta\mathbf{q}_c, \Delta\mathbf{q}_u$ as long as $\mathbf{T}_2$ is full rank. Rank deficiencies of $\mathbf{T}_2$, with $\mathbf{P}, \mathbf{U}$ full rank, are named *Type-2* singularities (as done in [8]). At the singular configuration, there exist non-null $\Delta\mathbf{q}_c, \Delta\mathbf{q}_u$ that leads to null $\Delta\mathbf{q}_a$. Practically, this means that in such configuration for certain motion of the legs and tubes displacement, there is no motors motion.

Moreover, Type 2 singularities are associated with changes in the stability pattern. Following the proof of [4], matrix $\mathbf{T}_2$ is singular if there exist a vector $\mathbf{u} \neq \mathbf{0}$ such as $\mathbf{Z}^T \begin{bmatrix} \mathbf{P}_1 & \mathbf{U}_1 \end{bmatrix} \mathbf{u} = \mathbf{0}$ and $\begin{bmatrix} \mathbf{P}_2 & \mathbf{U}_2 \end{bmatrix} \mathbf{u} = \mathbf{0}$. Since $\begin{bmatrix} \mathbf{P}_2 & \mathbf{U}_2 \end{bmatrix} = \mathbf{G}^T$ by definition, and the matrix $\mathbf{Z}$ spans the nullspace of $\mathbf{G}$, we have $\mathbf{u} = \mathbf{Z}\mathbf{v}$ for $\mathbf{v} \neq \mathbf{0}$. Thus, $\mathbf{T}_2$ is singular if there exist a vector $\mathbf{v} \neq \mathbf{0}$ such as $\mathbf{Z}^T \begin{bmatrix} \mathbf{P} & \mathbf{U} \end{bmatrix} \mathbf{Z}\mathbf{v} = \mathbf{H}^r\mathbf{v} = \mathbf{0}$, which proves that $\mathbf{T}_2$ is singular if $\mathbf{H}^r$ is singular. Additional details on the proof can be found in [4]. Other singularities may be investigated, such as rank deficiencies of $\mathbf{A}, \mathbf{U}, \mathbf{P}$ separately, but these considerations are not considered in this paper.

4 Case Study: two tubes *CTR*

In this section, we propose a case study with a two-tubes *CTR* to illustrate Type-1 and Type-2 singularities identification. We assume each tube to have

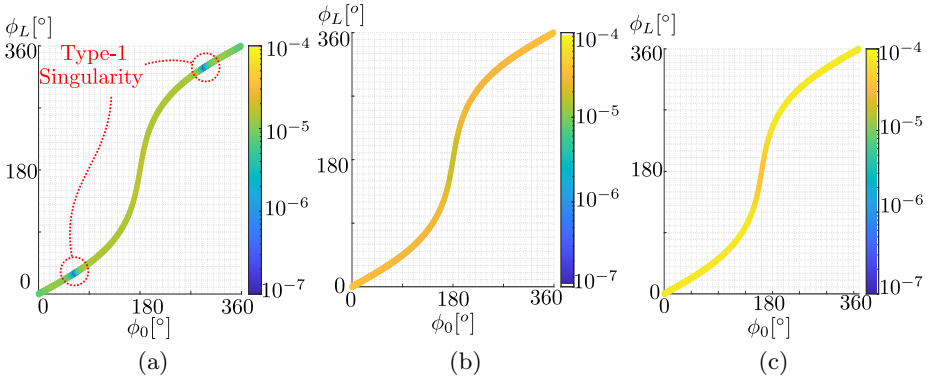

Fig. 2: S-curves obtained with $L = 0.4$m. Figures (a),(b) highlight the inverse conditioning of $\mathbf{T}_1, \mathbf{T}_2$, respectively, while figure (c) displays the minimum eigenvalue of $\mathbf{H}^r$

planar precurvature only, that is $\mathbf{u}_i^* = [u_{ix}^*, 0, 0]$, and both tubes perfectly overlapping with the same length $L = L_1 = L_2$. Moreover, we assume $\beta_1 = \beta_2 = 0$ for simplicity. We used NiTinol material parameters ($E = 80$ GPa), and we set $u_{1x}^* = 1/0.50\ m^{-1}$, $u_{2x}^* = 1/0.70\ m^{-1}$. The first tube has inner diameter d_{1inn} =1.0 mm, and outer diameter d_{1out} =1.5 mm, while the second tube has d_{2inn} =1.5 mm, and d_{2out} = 2.0 mm. Concerning the discretization strategy, we selected the piecewise constant strain approach of [14] for its simplicity, but the generality of the results holds with any discretization approach. We used 20 constant strain elements for each tube to achieve sufficient accuracy. We decide to parametrize $\mathbf{R}_p$ as $\mathbf{R}_p = \mathbf{R}_x(\alpha_1)\mathbf{R}_y(\alpha_2)\mathbf{R}_z(\alpha_3)$ with $\boldsymbol{\alpha} = [\alpha_1, \alpha_2, \alpha_3]^T$. Since we have two tubes, $\mathbf{q}_c \in \mathbb{R}^4$: we selected as controlled variables the tip position $\mathbf{p}_p$ and α_3, while $\mathbf{q}_d = [\alpha_1, \alpha_2] \in \mathbb{R}^2$.

The two-tube *CTR* case is a well-known situation where stability issues may occur. In this case, a global stability criterion was proposed in [10], which is based on the following inequality:

$$\zeta_\gamma = \frac{\cot(\gamma)}{\sqrt{\gamma}} < \zeta_{lim} \tag{16}$$

where

$$\gamma = L^2 u_{1x}^* u_{2x}^* \frac{k_{1b}k_{2b}(k_{1t}+k_{2t})}{k_{1t}k_{2t}(k_{1b}+k_{2b})}\ ,\ \zeta_{lim} = \frac{\beta_1 k_{2t} + \beta_2 k_{1t}}{L(k_{1t}+k_{2t})} \tag{17}$$

with k_{ib}, k_{it} the tubes stiffnesses as defined in Section 2. If the inequality of Eq. (16) is verified, than the *CTR* equilibrium is globally stable. A standard benchmark for *CTRs* equilibrium stability is based on the investigation of the *S-curves*: these curves describe the relation between the base orientations and the resulting *CTR* tip orientation, providing an intuitive representation of the robot motion abilities [10]. To build the *S-curve*, we fixed $\theta_{20} = 0$, and we

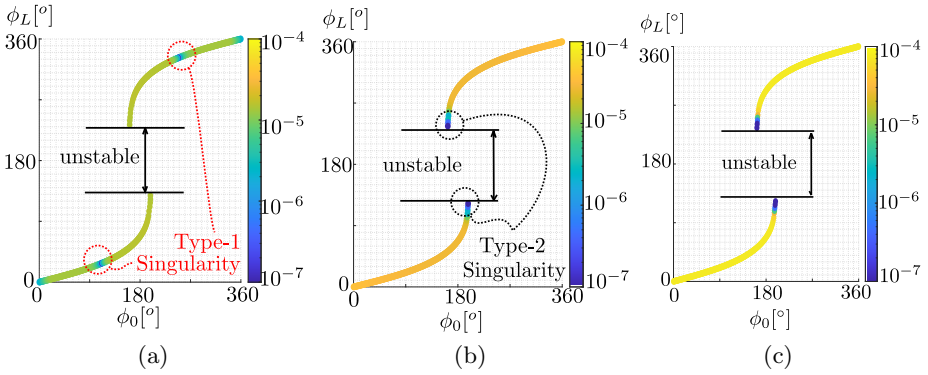

Fig. 3: S-curves obtained with $L = 0.6$m. Figures (a),(b) highlight the inverse conditioning of $\mathbf{T}_1, \mathbf{T}_2$, respectively, while figure (c) displays the minimum eigenvalue of $\mathbf{H}^r$

attempted to solve the forward problem with $\phi_0 = (\theta_{10} - \theta_{20}) \in [0, 2\pi]$. For each ϕ_0, we measured $\phi_L = (\theta_1(L) - \theta_2(L))$, and the inverse conditioning number k_{inv} of $\mathbf{T}_1, \mathbf{T}_2$ to detect Type-1 and Type-2 singularities, with the configuration considered singular if $k_{inv} < 10^{-6}$.

First, let us consider the case where $L = 0.4\ m$, which results in a globally stable equilibrium since $\zeta_\gamma = -0.164 < 0$. The resulting *S-curve* is reported in Fig. 2, and we highlighted Type-1 and Type-2 conditioning in Fig. 2(a), 2(b), respectively. By looking at Fig. 2(a), we can observe rank deficiencies of $\mathbf{T}_1$ at $\phi_0 = 54^\circ$ and 306°. At these configurations, there exist non-null $\Delta\mathbf{q}_a, \Delta\mathbf{q}_u$ that leads to null $\Delta\mathbf{q}_c$, meaning that the *CTR* tip cannot move along some desired controlled direction. On the contrary, no rank deficiency of $\mathbf{T}_2$ is found in Fig. 2(b), Type-2 singularities are not present, and the equilibrium is always stable all along the path since the minimum eigenvalue of $\mathbf{H}^r$ is always positive (Fig.2(c)). This is in accordance with the global stability criterion of Eq. (16): since Type-2 singularities delimits stable-to-unstable transitions and the equilibrium is globally stable, no Type-2 singularities should be present.

Different results are obtained when where $L = 0.6\ m$. In the case, $\zeta_\gamma = 0.242 \nleq 0$ and possible unstable transitions may occur. As before, we computed the *S-curve* (Fig. 3), and we highlighted Type-1 and Type-2 conditioning in Fig. 3(a), 3(b), respectively. Since $\zeta_\gamma > 0$, the *S-curve* is non monotonic, and the values of $\phi_L \in [128; 232]^\circ$ are associated with unstable equilibriums[6]. By varying L from 0.4 m to 0.6 m, degeneracies of $\mathbf{T}_1$ moved to $\phi_0 = 112^\circ$ and 248° (Fig. 3(a)), but the physical phenomena remains unchanged. Instead, Type-2 singularities are identified in Fig. 3(b), at $\phi_0 = 162^\circ$ and 198°. This is in

[6]Unstable configurations of the *S-curve* are not reachable with the solution of the forward problem. Other approaches, such as continuation techniques [13] offers an alternative tool for the scope.

accordance with state-of-the-art results [13], since Type-2 singularities appear where the slope of the *S-curve* is almost vertical, and a bifurcation point should be present [13]. At these configurations, there exist some non-null *CTR* motion even if the motors are braked, and the *CTR* equilibrium becomes unstable. We also verify that *Type-2* singularities correspond to equilibrium stability limits (Fig. 3(c)), since the inverse conditioning number of $\mathbf{T}_2$ tends toward zero when the minimum eigenvalue of $\mathbf{H}^r$ goes to zero as well.

5 Conclusions

In this paper, we introduced singularity conditions for *CTRs*. Based on the computation of the total *CTR* energy, we derived the *CTR* geometrico-static model by the use of discretization techniques, covering a wide range of currently used *CTRs* models. Then, we derived singularity conditions for the forward and inverse geometrico-static problems by linearization. Similarly to [4], we also shown the link between Type-2 singularities and *CTR* equilibrium stability. A case study with a two-tubes *CTR* was proposed to illustrate our results. By the study of the *S-curves*, we identified Type-1 singularities that correspond to the impossibility of the *CTR* to be moved in some controlled direction. We also identified Type-2 singularities that delimits stable-to-unstable regions. Future work will be directed toward the performance assessment and to the stability measurement of *CTRs*.

References

1. Alfalahi, H., Renda, F., Stefanini, C.: Concentric tube robots for minimally invasive surgery: Current applications and future opportunities. IEEE Transactions on Medical Robotics and Bionics **2**(3), 410–424 (2020)
2. Armanini, C., Boyer, F., Mathew, A.T., Duriez, C., Renda, F.: Soft robots modeling: A structured overview. IEEE Transactions on Robotics (2023)
3. Bergeles, C., Dupont, P.E.: Planning stable paths for concentric tube robots. In: 2013 IEEE/RSJ International Conference on Intelligent Robots and Systems, pp. 3077–3082. IEEE (2013)
4. Briot, S., Goldsztejn, A.: Singularity conditions for continuum parallel robots. IEEE Transactions on Robotics **38**(1), 507–525 (2021)
5. Burgner-Kahrs, J., Rucker, D.C., Choset, H.: Continuum robots for medical applications: A survey. IEEE Transactions on Robotics **31**(6), 1261–1280 (2015)
6. Chikhaoui, M.T., Rabenorosoa, K., Andreff, N.: Kinematics and performance analysis of a novel concentric tube robotic structure with embedded soft microactuation. Mechanism and Machine Theory **104**, 234–254 (2016)
7. Gilbert, H.B., Rucker, D.C., Webster III, R.J.: Concentric tube robots: The state of the art and future directions. In: Robotics Research: The 16th International Symposium ISRR, pp. 253–269. Springer (2016)
8. Gosselin, C., Angeles, J., et al.: Singularity analysis of closed-loop kinematic chains. IEEE transactions on robotics and automation **6**(3), 281–290 (1990)

9. Ha, J., Park, F.C., Dupont, P.E.: Elastic stability of concentric tube robots subject to external loads. IEEE Transactions on Biomedical Engineering **63**(6), 1116–1128 (2015)
10. Hendrick, R.J., Gilbert, H.B., Webster, R.J.: Designing snap-free concentric tube robots: A local bifurcation approach. In: 2015 IEEE International Conference on Robotics and Automation (ICRA), pp. 2256–2263. IEEE (2015)
11. Mahoney, A.W., Gilbert, H.B., Webster III, R.J.: A review of concentric tube robots: modeling, control, design, planning, and sensing. The Encyclopedia of Medical Robotics: Volume 1 Minimally Invasive Surgical Robotics pp. 181–202 (2019)
12. Nocedal, J., Wright, S.J.: Theory of constrained optimization. Numerical optimization pp. 304–354 (2006)
13. Peyron, Q., Rabenorosoa, K., Andreff, N., Renaud, P.: A numerical framework for the stability and cardinality analysis of concentric tube robots: Introduction and application to the follow-the-leader deployment. Mechanism and Machine Theory **132**, 176–192 (2019)
14. Renda, F., Cacucciolo, V., Dias, J., Seneviratne, L.: Discrete cosserat approach for soft robot dynamics: A new piece-wise constant strain model with torsion and shears. In: 2016 IEEE/RSJ International Conference on Intelligent Robots and Systems (IROS), pp. 5495–5502. IEEE (2016)
15. Renda, F., Messer, C., Rucker, C., Boyer, F.: A sliding-rod variable-strain model for concentric tube robots. IEEE Robotics and Automation Letters **6**(2), 3451–3458 (2021)
16. Rucker, C., Childs, J., Molaei, P., Gilbert, H.B.: Transverse anisotropy stabilizes concentric tube robots. IEEE Robotics and Automation Letters **7**(2), 2407–2414 (2022)
17. Rucker, D.C., Webster III, R.J., Chirikjian, G.S., Cowan, N.J.: Equilibrium conformations of concentric-tube continuum robots. The International journal of robotics research **29**(10), 1263–1280 (2010)
18. Webster, R.J., Romano, J.M., Cowan, N.J.: Mechanics of precurved-tube continuum robots. IEEE Transactions on Robotics **25**(1), 67–78 (2008)
19. Xu, K., Zhao, J., Geiger, J., Shih, A.J., Zheng, M.: Design of an endoscopic stitching device for surgical obesity treatment using a notes approach. In: 2011 IEEE/RSJ International Conference on Intelligent Robots and Systems, pp. 961–966. IEEE (2011)
20. Xu, R., Asadian, A., Naidu, A.S., Patel, R.V.: Position control of concentric-tube continuum robots using a modified jacobian-based approach. In: 2013 IEEE International Conference on Robotics and Automation, pp. 5813–5818. IEEE (2013)
21. Zaccaria, F., Briot, S., Chikhaoui, M.T., Idá, E., Carricato, M.: An analytical formulation for the geometrico-static problem of continuum planar parallel robots. In: Symposium on Robot Design, Dynamics and Control, pp. 512–520. Springer (2020)
22. Zaccaria, F., Idá, E., Briot, S., Carricato, M.: Workspace computation of planar continuum parallel robots. IEEE Robotics and Automation Letters **7**(2), 2700–2707 (2022)